



# Fermi National Accelerator Laboratory

FERMILAB-PUB-86/98-T

June, 1986

## Order $\alpha$ , QCD Effects in Technipion Production and Decay

**Douglas W. McKay**

The University of Kansas, Lawrence, Kansas 66045,  
and Fermi National Accelerator Laboratory,  
P.O. Box 500, Batavia, Illinois 60510

**Bing-lin Young and David Slaven**

Ames Laboratory and Department of Physics  
Iowa State University  
Ames, Iowa 50011

## ABSTRACT

The three-body final state decay modes of the technipion  $P^0$  which contribute as order  $\alpha$ , corrections to two-body modes are calculated. The three-body modes are large, and the three gluon final state is the dominant mode for  $M_{P^0} > 35$  GeV. Related effects in large  $p_\perp$  production of  $P^0$  in  $p$ - $p$  collision are calculated, and the cross-section at  $y = 0$  is found to be comparable to those of  $W^\pm$  and  $Z$  production at SSC energies but much smaller at Tevatron energies. It is pointed out that similar results should be expected for scalars in other models, such as the standard Higgs or compositeness models.



## Introduction

One approach to implementing dynamical breaking of weak interaction symmetry is that of the technicolor scheme,<sup>1</sup> where a non-abelian gauge interaction is postulated to exist and become strong at a scale of 1 TeV, where new physics is expected to emerge. The global chiral symmetry of the strong interaction Lagrangian is assumed to be spontaneously broken, and the  $W^\pm$  and  $Z$  bosons gain mass by the dynamical Higgs mechanism. The Higgs sector of the standard model is replaced by the pseudo-Goldstone bosons which are pseudoscalar excitations arising from the dynamical chiral symmetry breaking. The pseudoscalars which are not absorbed by the Higgs mechanism become massive in the presence of  $SU(3) \times SU_L(2) \times U(1)$  interactions and the extended technicolor interactions between light fermions and heavy (techni) fermions.<sup>2</sup> These would-be Goldstone bosons are the lowest mass states in such a picture and are referred to as technipions.

In any model in which there are several technifermion doublets, there is at least one set of four color-singlet technipions, a weak isosinglet and an isodoublet,<sup>2</sup> which gain mass only from electroweak and/or from extended technicolor interactions. These states, called  $P^\pm$ ,  $P^0$  and  $P^{0'}$ , are expected to be the lightest of all the technipions. Because these particles are the least model dependent, they provide a decisive testing ground of technicolor dynamical symmetry breaking. The only weak link is that the couplings to light fermions and the precise values of these technipion masses are model dependent. Estimates place their mass values in the range from 10 to 40 GeV.<sup>2,3</sup> The couplings of the technipions to the standard model  $SU(3) \times SU_L(2) \times U(1)$  gauge bosons, on the other hand, are completely determined by the minimal gauging by covariant derivatives for the normal parity, non-anomalous interactions, and by minimal anomaly structure for the anomaly driven, abnormal parity interactions (those involving the epsilon tensor). The latter are parametrized by the standard model gauge couplings, the dimensionality  $N_T$  of the technifermion representations in the technicolor group, and the technipion decay constant  $F_T$ .

The weak iso-singlet particle  $P^{0'}$  has anomalous, purely gluonic interactions which give it substantial decay and production channels apart from the rather model dependent fermion-antifermion channels which control the  $P^\pm$  and  $P^0$  decays. The  $P^{0'}$  fermion-antifermion coupling is expected to be dominated by the  $b\bar{b}$  channel if the usual coupling pattern, proportional to the fermion mass, holds true here.

Therefore the dominant two-body channels are  $b\bar{b}$  and two gluons in the  $P^{o'}$  case. Because of the lightness of this particle, which could possibly be produced and detected in existing accelerators and certainly in the next generation accelerators, and because of its sharing certain common properties with the standard Higgs particle, the production and decay of  $P^{o'}$  merits a detailed study.

In this paper we examine the order  $\alpha_s$ , quantum chromodynamics (QCD) corrections to the lowest order  $P^{o'}$ -2 gluon ( $P^{o'}gg$ ) and  $P^{o'}$ -2b quark ( $P^{o'}b\bar{b}$ ) vertices, calculating the corresponding three-body final state branching ratios and the large transverse momentum ( $p_\perp$ ) production of the  $P^{o'}$  particle. This study supplements previous work on  $P^{o'}$  two-body decays and production by gluon fusion,<sup>3</sup> complementing the pair production of  $P^\pm$  in  $e^+e^-$  collisions as tests of technicolor. It is known from QCD that order  $\alpha_s$  effects can be sizeable in certain processes,<sup>4</sup> and we will show below that they are important in the discussion of  $P^{o'}$  physics. The order  $\alpha_s$  corrections strongly affect branching fractions and production channels and, furthermore, are similar for any flavor singlet and color singlet scalar particle which decays to fermion-antifermion pairs and to two gluons. Therefore the general issues in our discussion apply to any model which contains such scalars, including those such as the standard Higgs particle and composite model scalars. The values of the total decay rate and the production cross-sections depend upon the pseudoscalar character of the technipion as well as the model-dependent values of  $N_T$  and  $F_T$ , of course. For numerical evaluations we use  $N_T = 4$  and  $F_T = 125$  GeV, as in the one generation Farhi-Susskind model.<sup>1,5</sup>

The main features of our results are that the 3-gluon decay mode of  $P^{o'}$  is comparable to the 2-gluon mode for small ( $\lesssim 20$  GeV)  $P^{o'}$  mass and dominates all other modes for large ( $\gtrsim 40$  GeV) mass and that the production cross-section of  $P^{o'}$  in proton-proton ( $p$ - $p$ ) collisions at large  $p_\perp$  and small rapidity ( $y \approx 0$ ) is comparable to those of  $W$  and  $Z$ .<sup>6,7</sup> We note that the  $P^{o'}$  production falls less steeply with  $p_\perp$  than for  $W$  and  $Z$  production and increases more rapidly with the reaction energy.

## Discussion of Order $\alpha_s$ Effects

Decay modes of  $P^{o'}$  which have been treated in Refs. 3 and 6 are  $P^{o'} \rightarrow b\bar{b}$  and  $P^{o'} \rightarrow gg$ . The latter process is used<sup>3,6</sup> to estimate  $P^{o'}$  production by gluon fusion,

and the comparison of the subsequent  $P^{o'} \rightarrow b\bar{b}$  decay to the QCD background production of heavy quark pairs is made. Here we calculate the “gluonic Dalitz pair” decay modes  $P^{o'} \rightarrow q\bar{q}g$ , where  $q$  denotes the light quarks  $u, d, s$ , and  $c$ , the gluon brehmstrahlung  $P^{o'} \rightarrow b\bar{b}g$ , and the three gluon mode  $P^{o'} \rightarrow ggg$  and the related parton production processes  $gq \rightarrow P^{o'}q$ ,  $q\bar{q} \rightarrow P^{o'}g$  and  $gg \rightarrow P^{o'}g$ . These production processes are responsible for transverse, large  $p_\perp$  production of  $P^{o'}$  in  $p$ - $p$  and  $p$ - $\bar{p}$  collisions. In contrast to the ordinary Dalitz pair modes  $\pi^0 \rightarrow \gamma e^+ e^-$  and  $\eta \rightarrow \mu^+ \mu^- \gamma$ , which have small branching ratios, the gluonic Dalitz pair mode in the present case is sizable (order 5%).

In principle all of the relevant vertices are contained in the effective, chiral Lagrangian of pseudo-Goldstone bosons of a global chiral symmetry spontaneously broken by technicolor condensates, where the effects of chiral anomalies can be summarized in a Wess-Zumino type of effective action.<sup>8,9</sup> For present purposes it suffices to use published results for three point vertices<sup>10,3,6</sup> and the QCD  $ggg$  and  $\bar{q}qg$  couplings. The one exception is the contact term  $P^{o'}ggg$ , shown in Fig. 1. as one of the four Feynman graphs of order  $g_s^3$  which contribute to the  $P^{o'}ggg$  amplitude. The value of this contact term is uniquely determined by gluon gauge invariance and Bose symmetry, however, so one does not need the full Wess-Zumino anomalous action to get it.<sup>9</sup> The  $P^{o'}$  decay into three gluons and the  $P^{o'} + g$  production by gluon fusion in  $p$ - $p$  collision are indicated in Figs. 1 and 2, respectively.

### Three-body Decay Modes at Order $\alpha_s^3$

We have computed the decay rates for  $P^{o'} \rightarrow ggg$ ,  $P^{o'} \rightarrow b\bar{b}g$ ,  $P^{o'} \rightarrow gq\bar{q}$  and we plot the branching fractions as a function of mass, along with the  $b\bar{b}$ ,  $\tau\bar{\tau}$  and  $gg$  rates from Ref. 3, in Fig. 3. A fixed value of  $\alpha_s = 0.2^{11}$  was used in the calculations leading to Fig. 3, and a minimum invariant mass cutoff of 4 GeV invariant mass was used for the  $gg$  and  $q\bar{q}$  subchannels in the  $3g$  and the  $gq\bar{q}$  (Dalitz pair) final states,<sup>12</sup> while a minimum of 7 GeV was imposed on the  $bg$  and  $\bar{b}g$  invariant masses in the  $b\bar{b}g$  channel (corresponding to a minimum gluon energy of 1.7 GeV). We have tried a variety of cutoff values as well as letting  $\alpha_s$  run as a function of the relevant propagator’s invariant mass in the  $b\bar{b}g$  and  $gq\bar{q}$  calculations, but the results of the total width and relative branching fractions change by at most 50% among the various cases.<sup>13</sup> The results shown in Fig. 3 are approximately in the middle of the

range of three-body decay rates which we found. As is clear from Fig. 3, the three-body final states contribute significantly to the decay rate of the  $P^{o'}$ , increasing its width by a factor 1.3 for  $M_{P^{o'}} = 20 \text{ GeV}$  and by a factor 3 for  $M_{P^{o'}} = 50 \text{ GeV}$ , largely due to the  $3g$  channel. This result affects any estimate of the number of  $P^{o'}$  events in a given channel, since the production cross-section times the branching fraction is the relevant quantity. In particular, the branching fraction into  $\bar{b}b$  is a factor 2-3 less than previously estimated<sup>3</sup> for  $M_{P^{o'}} \gtrsim 40 \text{ GeV}$  when only two body decay modes were considered.

### Order $\alpha_s$ Corrections to $P^{o'}$ Production

As in the case of weak boson production in  $p$ - $p$  collisions, order  $\alpha_s$  corrections to  $P^{o'}$  production are important and lead to substantial transverse production of  $P^{o'}$ , which recoils against a quark or a gluon jet. The production process is shown schematically for  $g + P^{o'}$  production in Fig. 2, and the sub-process cross-sections,  $\hat{\sigma}$ , for  $g + g \rightarrow g + P^{o'}$ ,  $g + q(\bar{q}) \rightarrow P^{o'} + q(\bar{q})$  and  $q\bar{q} \rightarrow P^{o'} + g$  which we have calculated are presented in the Appendix. In Fig. 4 we show the quantity  $\frac{d^2\sigma}{dp_\perp dy}\big|_{y=0}$  as a function of  $p_\perp$  at  $\sqrt{s} = 2 \text{ TeV}$ ,  $40 \text{ TeV}$  and  $100 \text{ TeV}$ .<sup>14</sup> The dependence on  $M_{P^{o'}}$  is negligible for  $p_\perp > 100 \text{ GeV}$  and gives at most 30% variations for  $20 \text{ GeV} \leq M_{P^{o'}} \leq 60 \text{ GeV}$  for  $p_\perp < 100 \text{ GeV}$ . The corresponding  $W^\pm$  production (sum of  $W^+ + W^-$ ) is also shown for comparison.<sup>15</sup> The  $Z^0$  production is roughly half of the  $W^\pm$  production.<sup>16</sup> The  $P^{o'}$  production has both a "stiffer" dependence on  $P_\perp$  and a faster increase as a function of the reaction energy than those of  $W^\pm$ . This is due to the extra momentum dependence in the anomalous  $P^{o'}gg$  vertex compared to the  $W$ -quark couplings which enter in the weak boson amplitudes. On the basis of an SSC design of an integrated luminosity of  $10^7 (\text{nb})^{-1}$  at  $\sqrt{s} = 40 \text{ TeV}$ , one can estimate that on the order of  $10^4 P^{o'}$ 's would be produced in the range  $0.4 \text{ TeV} < P_\perp < 0.8 \text{ TeV}$  in the rapidity range  $-\frac{1}{2} \leq Y \leq \frac{1}{2}$ . The  $\bar{b}b$  and  $\bar{\tau}\tau$  decay signals, with recoil against a jet, are probably the clearest ones for identifying a  $P^{o'}$ . The branching fraction to these channels is quite dependent on  $M_{P^{o'}}$ , as is shown in Fig. 3, and generally smaller than in previous estimates which ignored the 3-body final states. On balance, however, we feel that the substantial transverse  $P^{o'}$  production which we calculate due to the  $\alpha_s$  corrections to simple gluon fusion enhances the prospects for detecting  $P^{o'}$  at the Tevatron or SSC.

## Remarks on Other Neutral, Spin Zero Particles

Since the technicolor scheme simulates the standard model at low energies, it is no surprise that the behavior of  $P^{\circ'}$  and the standard model Higgs boson,  $H^{\circ}$ , have similar behavior at similar mass values. If a color singlet, scalar particle is discovered with a mass much larger than 40 GeV, then it is very likely to be a Higgs boson or a composite scalar. If, on the other hand, the mass is in the 50 GeV range expected for technipions, means have to be found to distinguish among different interpretations. The various decay widths of the single Higgs of the standard model have been calculated in Ref. 17, which allows us to compare the  $H^{\circ}$  and  $P^{\circ'}$  for the  $2\gamma$ ,  $2g$  and  $b\bar{b}$  modes: the ratios of the  $P^{\circ'}$  decay widths to those of the  $H^{\circ}$  are, respectively for the three modes, 2.3, 7.4 and 0.55 when the scalar mass is 20 GeV, and 2.2, 5.2 and 0.16 for a mass of 40 GeV. An example of the ambiguity that can arise is given by the case of scalar production by gluon fusion and subsequent decay into  $b\bar{b}$ . The  $H^{\circ}$  production by gluon fusion is suppressed compared to  $P^{\circ'}$ , but its branching fraction to  $b\bar{b}$  is larger than that of  $P^{\circ'}$ . Differences between  $H^{\circ}$  and  $P^{\circ'}$  tend to wash out in the product of cross-section  $\times$  branching ratio.

Other types of scalars,  $H^{\circ'}$ , which may appear in composite models are also discussed in Ref. 17. An important property of these latter scalar bosons is their possibility of having large  $2\gamma$  rates which can be searched for in  $e^+e^-$  collision in the three photon final state in the reaction  $e^+e^- \rightarrow (\gamma, Z) \rightarrow H^{\circ'} + \gamma \rightarrow 3\gamma$ .<sup>17</sup>

## Conclusions

We conclude from our study that order  $\alpha_s(Q^2)$  effects in  $P^{\circ'}$  technipion production and decay are important and must be included to assess accurately the  $P^{\circ'}$  characteristics. We expect the same conclusions to hold in the case of standard model Higgs scalars and in the case of scalars in composite models. We found that technipion production at large  $p_{\perp}$  is smaller than  $W$ -production at the lower range of  $p_{\perp}$  values and as large as  $W$ -production at higher  $p_{\perp}$  values. Three-body decay modes of the technipion are comparable to the two body modes, ranging from 30% to 300% of the two body decay rate as the mass ranges from 15 GeV to 60 GeV. This fact is important for assessing the observability of given final states in the decay of  $P^{\circ'}$ .

Because the effects which we calculated are relevant also to scalar particles in other kinds of symmetry breaking schemes, and the signals of scalar production and decay in different schemes are somewhat similar, we feel that a detailed survey of the comparative features of the scalars is needed, including details of the effects which we have described, in order to find unambiguous tests for the nature of new particle and Higgs boson candidates in future experiments.

### Acknowledgements

This work was completed while one of the authors (B.-L.Y.) was participating in the Argonne National Laboratory Informal Summer Institute on Superstrings. He would like to thank Cosmas Zachos for partial financial support and for hospitality extended to him at the workshop. Doug McKay thanks Chris Quigg and the rest of the theory group at Fermilab for hospitality during his sabbatical leave while this work was done. This work is supported in part by the Department of Energy under contract number W-7405-Eng-84, Office of Basic Science [KA-01-01], Division of High Energy Physics and Nuclear Physics, and grant No. DE-FG02-85ER 40214.

### Appendix

Here we list the subprocess cross-sections,  $\hat{\sigma}(\hat{s}, \hat{t}, \hat{u})$ , which are used to calculate the  $P^{o'}$  production cross-sections shown in Fig. 4.

1.  $q + \bar{q} \rightarrow g + P^{o'}$ :

$$\hat{\sigma}(\hat{s}, \hat{t}, \hat{u}) = \frac{\alpha_s^3(Q^2)}{108\pi^2 F_T^2} \frac{(\hat{t}^2 + \hat{u}^2)}{\hat{s}^2},$$

where  $\hat{t}$ ,  $\hat{s}$ , and  $\hat{u}$  are the sub-process Mandelstam variables.

2.  $g + q(\bar{q}) \rightarrow P^{o'} + q(\bar{q})$ :

$$\hat{\sigma}(\hat{s}, \hat{t}, \hat{u}) = \frac{\alpha_s^3(Q^2)}{288\pi^2 F_T^2} \left[ \frac{2m_p^2 \hat{s} \hat{u} + (\hat{s} + \hat{u})(\hat{s}^2 + \hat{u}^2 - m_p^2(\hat{s} + \hat{u}))}{\hat{s} \hat{t}^2} \right],$$

where  $\hat{t}$  is the  $g - P^{o'}$  invariant momentum transfer.

3.  $g + g \rightarrow P^{o'} + g$ :

$$\hat{\sigma}(\hat{s}, \hat{t}, \hat{u}) = \frac{\alpha_s^3(Q^2)}{64\pi^2 F_T^2} \times \frac{1}{\hat{s}} \left\{ m_p^2 \left[ 1 + m_p^2 \left( \frac{1}{\hat{u}} + \frac{1}{\hat{t}} + \frac{1}{\hat{s}} \right) + \frac{\hat{s}^2}{\hat{u}\hat{t}} + \frac{\hat{u}^2}{\hat{s}\hat{t}} + \frac{\hat{t}^2}{\hat{s}\hat{u}} \right] + \frac{\hat{u}\hat{t}}{\hat{s}} + \frac{\hat{s}\hat{t}}{\hat{u}} + \frac{\hat{s}\hat{u}}{\hat{t}} \right\}$$

The amplitude for the process shown in Fig. 1, used in obtaining  $\hat{\sigma}$  for case 3 above (by crossing) and for  $P^{o'} \rightarrow 3g$  decay, is

$$\begin{aligned} \mathcal{M}(P^{o'}(p) \rightarrow g^a(k_1) + g^b(k_2) + g^c(k_3)) = \\ \frac{g_s^3 N_T f^{abc}}{16\pi^2 \sqrt{3} F_T} \epsilon^{\mu\lambda\sigma\nu} \left\{ -\epsilon_\mu(k_1) \epsilon_\lambda(k_2) \epsilon_\sigma(k_3) p_\nu \right. \\ + \frac{1}{(k_2 + k_3)^2} [g_{\mu\rho}(2k_2 + k_3)_\tau + g_{\rho\tau}(k_3 - k_2) + g_{\tau\mu}(-k_2 - 2k_3)_\rho] \epsilon^\rho(k_2) \epsilon^\tau(k_3) \\ \left. + 1 \leftrightarrow 2, \rho \leftrightarrow \mu, a \leftrightarrow b + 1 \leftrightarrow 3, \tau \leftrightarrow \mu, a \leftrightarrow c \right\}. \end{aligned}$$

## References and Footnotes

1. S. Weinberg, Phys. Rev. *D13*, 974 (1976); *D19*, 1277 (1979); L. Susskind, Phys. Rev. *D20*, 2619 (1979). For a review, see E. Farhi and L. Susskind, Phys. Rep. *74*, 277 (1981).
2. S. Dimopoulos and L. Susskind, Nucl. Phys. *B155*, 237 (1979); E. Eichten and K. Lane, Phys. Lett. *90B*, 125 (1980).
3. E. Eichten, I. Hinchliffe, K. Lane and C. Quigg, "Signatures for Technicolor", Fermilab-Pub. 85/145-T (1985).
4. An example is quark pair plus gluons modes in quarkonium decay: R. Barbieri, M. Caffo and E. Remiddi, Phys. Lett. *89B*, 345 (1979).
5. E. Farhi and L. Susskind, Phys. Rev. *D20*, 3404 (1979).
6. E. Eichten, I. Hinchliffe, K. Lane and C. Quigg, Rev. Mod. Phys. *56*, 579 (1984).
7. G. Altarelli, R. Ellis and G. Martinelli, Z. Phys. C, *27*, 617 (1985).

8. J. Wess and B. Zumino, Phys. Lett. *37B*, 95 (1971); E. Witten, Nucl. Phys. *B223*, 422 (1983).
9. For application to technicolor see D. McKay and B.-L. Young, Phys. Lett. *169B*, 79 (1986).
10. S. Dimopoulos, S. Raby and G. L. Kane, Nucl. Phys. *B182*, 77 (1981); J. Ellis, M. K. Gaillard, D. V. Nanopoulos and P. Sikivie, Nucl. Phys. *B182*, 529 (1981).
11.  $\alpha = 0.2$  corresponds to  $Q = 8.6$  GeV in the four-flavor case or  $Q = 12.0$  GeV for five flavors, where the QCD scale parameter is set at  $\Lambda = 0.2$  GeV.
12. An invariant mass cutoff of 4 GeV is a rather large one. See, for example, K. Fabricius et al., Phys. Lett. *97B*, 431 (1980). This cutoff obviates the need to consider virtual gluon corrections.
13. The use of a running  $\alpha_s(Q^2)$  is not so simple in the case of the three gluon mode. One cannot identify  $Q$  as the virtual gluon mass in the diagrams of Fig. 1 which involve the gluon trilinear coupling. The virtual gluon masses in the three diagrams are generally different in a given kinematical configuration and therefore the three  $\alpha_s(Q^2)$ 's are different. But gauge invariance requires them to be the same. The identification of  $Q$  with the invariant mass of any pair of gluons for the contact term of Fig. 1 is not allowed because of Bose symmetry.
14. In order to compare directly with results published in Ref. 6, we use their set of one structure functions in displaying the results in Fig. 4. Using the structure functions of J. Collins and W.-K. Tung, Fermilab-Pub-86/39-T, one would expect results which are slightly smaller at  $p_\perp < 100$  GeV. We thank Wu-Ki Tung for instruction in and use of his flexible structure function program [see *Proceedings of the Workshop on Physics Simulations at High Energy*, Madison, 1986.]
15. We use the sum of  $W^+$  and  $W^-$  production cross-sections as given in, eg. Refs 6 and 7 (denoted  $d\sigma(W^\pm)$ ). We also calculated  $d\sigma(W^-)$  separately using the EHLQ parton distribution functions as compiled in Ref. 14. We found that  $d\sigma(W^\pm)/d\sigma(W^-)$  is slightly greater than 2 at small  $p_\perp$ . The ratio increases with  $p_\perp$ . For example, at  $\sqrt{s} = 40$  TeV, the ratio is 2.06 at  $p_\perp = 0.05$  TeV and

at  $p_{\perp} = 1.2$  the ratio is 2.65. Our  $d\sigma(W^{\pm})$  checks with that of EHLQ, Ref. 6. We thank C. Quigg and E. Eichten for providing us with the corrected version of  $d\sigma(W^{\pm})$  [Ref. 6 Errata, to be published].

16. A review of the various calculations is given in R. Peccei in *Techniques and Concepts of High Energy Physics, III*, T. Ferbel, Ed., Plenum, New York (1985). See also Ref. 6.
17. K. Whisnant, B.-L. Young and S. Hu, Phys. Rev. *D31*, 1566 (1985).

### Figure Captions

- Figure 1: Feynman diagrams for  $P^{\circ'} \rightarrow ggg$  decay.
- Figure 2: Parton-model graph of gluon-gluon fusion contribution to large  $p_{\perp}$  production of  $P^{\circ'}$  in  $p$ - $p$  collision.
- Figure 3: Plot of branching ratios (B.R.) vs. mass of  $P^{\circ'}$  of decay into  $\tau\bar{\tau}$  (unlabeled solid),  $q\bar{q}g$  ( $q = u, d, s, c$ ) (unlabeled dash-dotted),  $b\bar{b}g$  (unlabeled dotted),  $gg$  (unlabeled dashed)  $b\bar{b}$  and  $ggg$ .
- Figure 4: Plot of  $\frac{d\sigma}{dp_{\perp}dy}$  at  $y = 0$  of  $W^{\pm}$  production (dashed) and  $P^{\circ'}$  production (solid) at  $\sqrt{s} = 2, 40$  and  $100$  TeV.

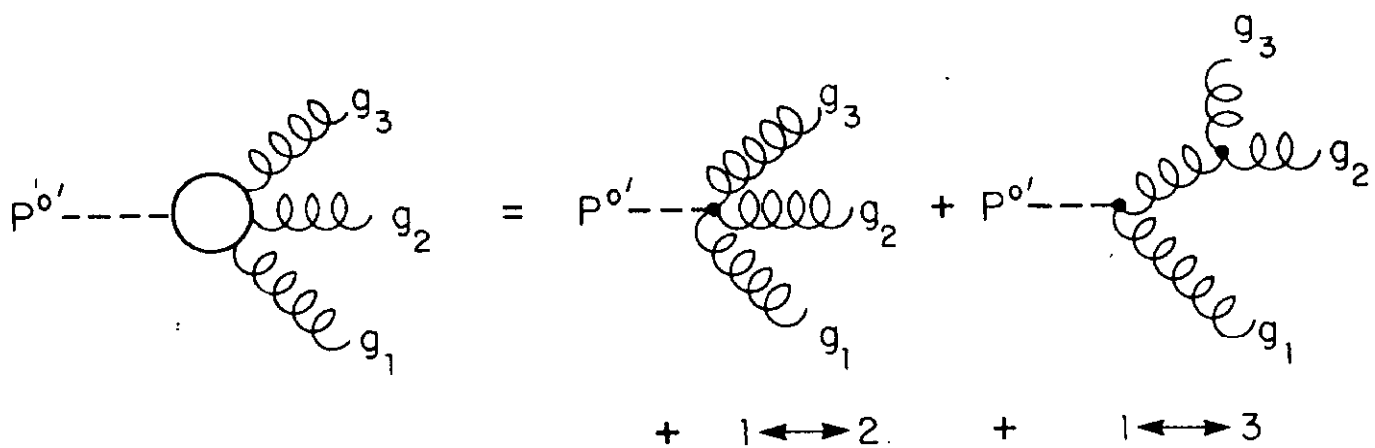


Figure 1: Feynman diagrams for  $P^{o'} \rightarrow ggg$  decay.

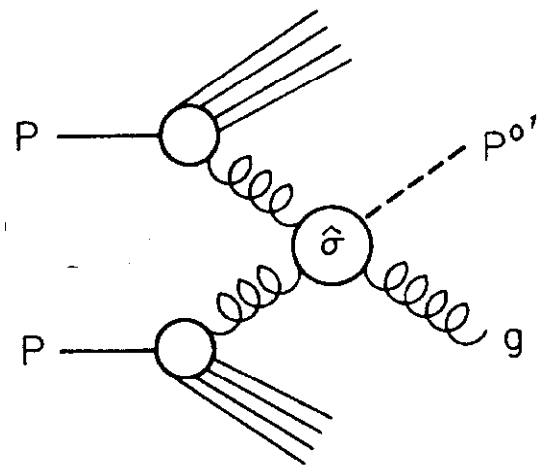


Figure 2: Parton-model graph of gluon-gluon fusion contribution to large  $p_{\perp}$  production of  $P^{0'}$  in  $p$ - $p$  collision.

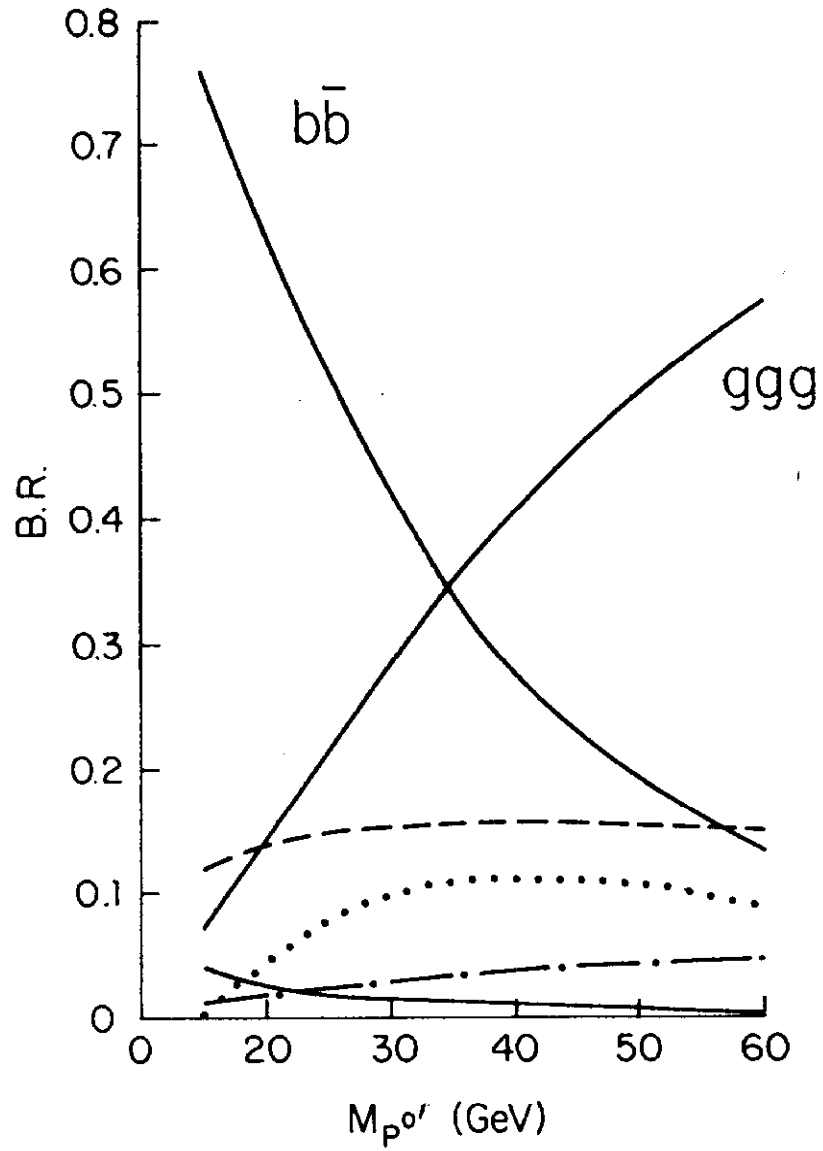


Figure 3: Plot of branching ratios (B.R.) vs. mass of  $P^{0'}$  of decay into  $r\bar{r}$  (unlabeled solid),  $q\bar{q}g$  ( $q = u, d, s, c$ ) (unlabeled dash-dotted),  $b\bar{b}g$  (unlabeled dotted),  $gg$  (unlabeled dashed)  $b\bar{b}$  and  $ggg$ .

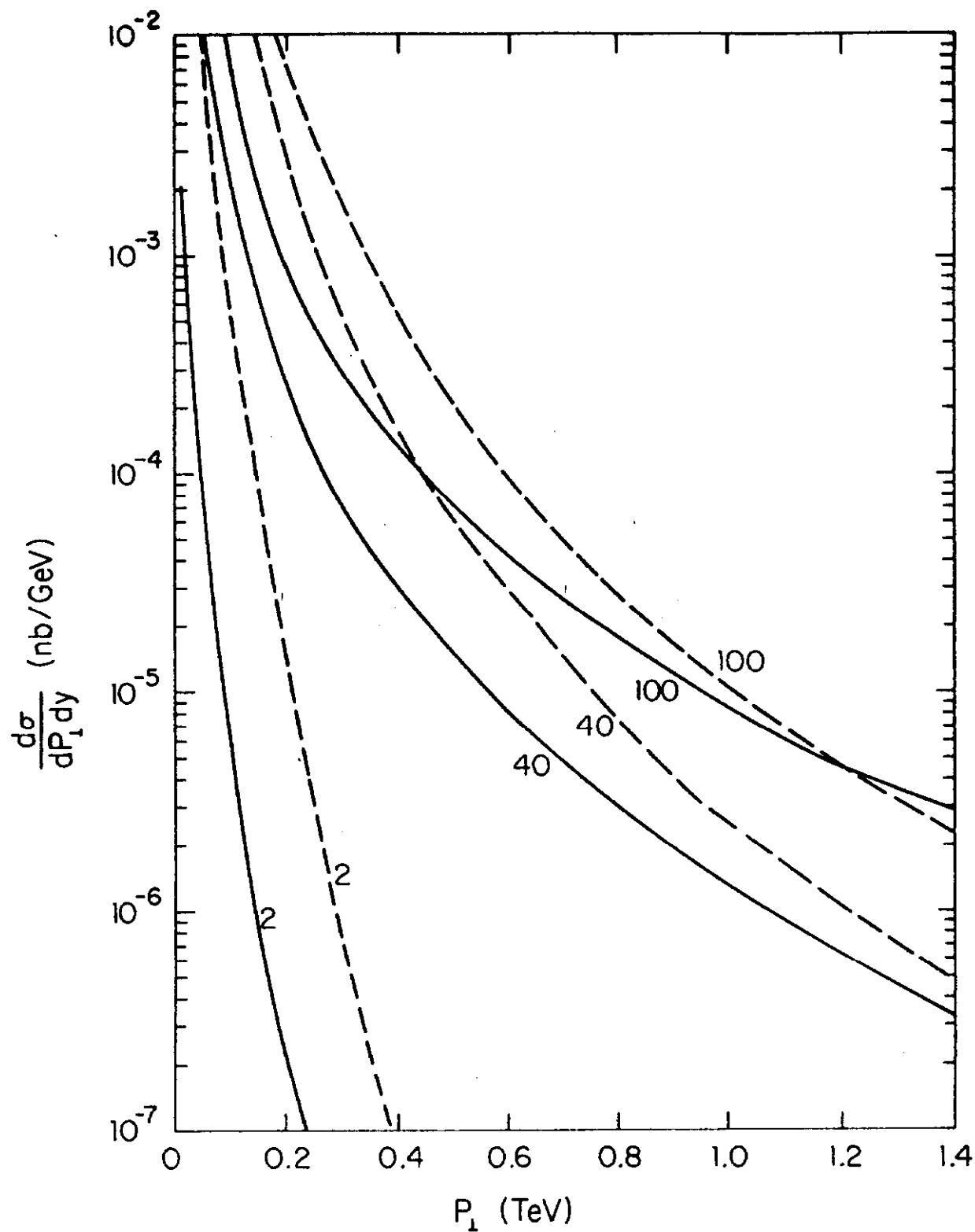


Figure 4: Plot of  $\frac{d\sigma}{dp_{\perp}dy}$  at  $y = 0$  of  $W^{\pm}$  production (dashed) and  $P^{\circ'}$  production (solid) at  $\sqrt{s} = 2, 40$  and  $100$  TeV.